Finite-Size Scaling and Particle-Size Cutoff Effects in Phase-Separating Polydisperse Fluids

Nigel B. Wilding
Department of Physics, University of Bath, Bath BA2 7AY, United Kingdom

Peter Sollich and Moreno Fasolo
King's College London, Department of Mathematics, Strand, London WC2R 2LS, United Kingdom
(Received 8 July 2005; published 6 October 2005)

We study the liquid-vapor phase behavior of a polydisperse fluid using grand canonical simulations and moment free energy calculations. The strongly nonlinear variation of the fractional volume of liquid across the coexistence region prevents naive extrapolation from detecting the cloud point. We describe a finite-size scaling method which, nevertheless, permits accurate determination of cloud points from simulations of a single system size. By varying a particle-size cutoff, we find that the cloud point density is highly sensitive to the presence of rare large particles; this could affect the reproducibility of experimentally measured phase behavior in colloids and polymers.

DOI: 10.1103/PhysRevLett.95.155701 PACS numbers: 64.70.Fx, 68.35.Rh

Many complex fluids such as colloidal dispersions, liquid crystals, and polymer solutions are inherently polydisperse in character: their constituent particles have an essentially continuous range of size, shape, or charge. Polydispersity is of significant practical importance because it can affect material properties in applications ranging from coating technologies and foodstuffs to polymer processing [1]. However, our understanding of the fundamental properties of polydisperse fluids remains very limited compared with what we know about their monodisperse counterparts. The challenge arises because a polydisperse fluid is effectively a mixture of an *infinite* number of particle species. Labeling each by the value of its polydisperse attribute σ, the state of the system (or any of its phases) has to be described by a density *distribution* $\rho(\sigma)$, with $\rho(\sigma)d\sigma$ the number density of particles in the range $\sigma, \ldots, \sigma + d\sigma$. The most common experimental situation is that in which the form of the overall or ''parent'' distribution $\rho^0(\sigma)$ is fixed by the synthesis of the fluid, and only its scale can vary depending on the proportion of the sample volume occupied by solvent. One can then write $\rho^0(\sigma) = n^0 f^0(\sigma)$ where $f^0(\sigma)$ is the normalized parent shape function and $n^0 = N/V$ the overall particle number density. Varying n^0 at a given temperature corresponds to scanning a ''dilution line'' of the system.

A central issue in the physics of polydisperse fluids is the nature of their phase behavior: in order to process a polydisperse fluid one needs to know under which conditions it will demix and what phases will result. However, the phase behavior of polydisperse systems can be considerably richer than that of monodisperse systems, due to the occurrence of *fractionation* [2–4]: at coexistence, particles of each σ may partition themselves unevenly between two or more ''daughter'' phases as long as—because of particle conservation—the overall density distribution $\rho^0(\sigma)$ of the parent phase is maintained. As a consequence, the conventional fluid-fluid binodal of a monodisperse system splits into a cloud curve marking the onset of coexistence, and a shadow curve giving the density of the incipient phase; the critical point appears at the intersection of these curves rather than at the maximum of either [5].

In this Letter we describe a joint simulation and theoretical study of a model polydisperse Lennard-Jones fluid in which the size of the particles influences not only the length-scale but also the strength ϵ_{ij} of the interparticle potentials, as defined in (2) below. For the case of size-independent interaction strengths, the critical point lies very close to the maximum of the cloud curve [6], whereas for the present model we find that it is substantially below, as is observed in many experiments on complex fluids (see, e.g., [7]) and simplified theoretical calculations [8]. At the critical temperature, T_c, there then exists a finite density range where phase separation occurs on the dilution line. Most results shown below are at this temperature; note that we are interested mainly in the low-density part of the coexistence region rather than the critical effects at the other end, using T_c merely as a convenient temperature scale.

The simulations were performed within the grand canonical ensemble (GCE). This is particularly useful for polydisperse systems, where it permits sampling of many different realizations of the particle-size distribution while catering naturally for fractionation effects. Operationally, we ensure that the ensemble averaged density distribution always equals the desired parent form $\rho^0(\sigma)$ by controlling an imposed chemical potential distribution $\mu(\sigma)$. A combination of novel and existing techniques [9] are required to tune $\mu(\sigma)$ such as to track the dilution line, i.e., to vary the parent density n^0 but not its shape $f^0(\sigma)$.

In the GCE simulations, the number density n is a fluctuating variable with average equal to n^0. Its distribution $p(n)$, shown in Fig. 1 for a range of parent densities n^0 at $T = T_c$, is a key observable. In the coexistence region it has two distinct peaks, which we sample using multica-

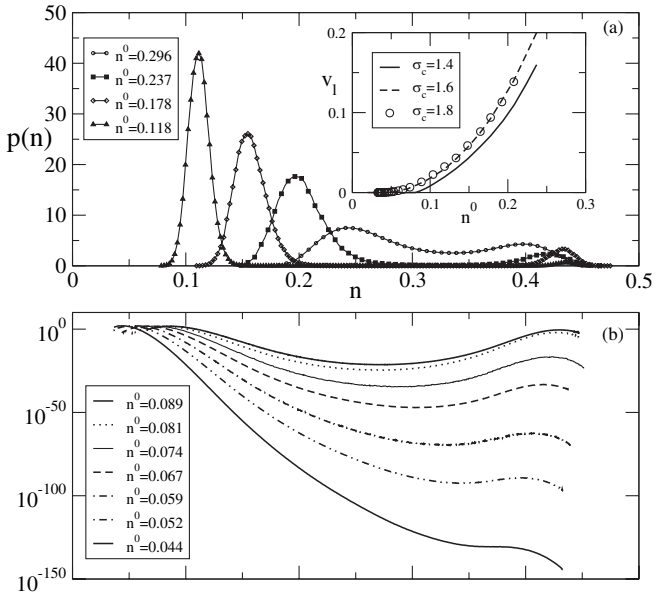

FIG. 1. Number density distribution $p(n)$ at $T = T_c$ for parent densities n^0 as indicated and for particle-size cutoff $\sigma_c = 1.4$. The system size is $L = 15\bar{\sigma}$. See text after Eq. (2) for definitions of σ_c and $\bar{\sigma}$. (a) Linear and (b) log scale. Inset: Liquid fractional volume v_l versus n^0, for $\sigma_c = 1.4, 1.6, 1.8$.

nonical preweighting [10]. The weight under the low and high density peaks corresponds, respectively, to the fractional volumes v_g and v_l that would be occupied by gas and liquid in the corresponding canonical ensemble. As expected, the peaks separate and the valley between them deepens as we move away from the critical point by decreasing n^0. Concomitant with this is a gradual transfer of weight from the liquid to the gas peak. Finally the liquid peak disappears, at exponentially small values of v_l visible only on a log scale [Fig. 1(b)].

The observed variation of $p(n)$ raises the question of how to detect the cloud point n^0_{cl}, defined as the lowest parent density n^0 where stable phase coexistence occurs. In a monodisperse system this is straightforward because the cloud point also gives the density of the gas phase, which remains constant throughout the coexistence region. One then simply detects the point where the gas and liquid peaks have the same weight, i.e., $r = v_l/v_g = 1$, and measures the gas density there. (This equal peak weight criterion has the added advantage of leading to only exponentially small finite-size corrections to the value of μ at coexistence [11].) However, this method fails in a polydisperse system because fractionation causes the densities and size distributions of the coexisting phases to vary with n^0 [5]. One could attempt to locate the cloud point instead by extrapolating in n^0 to the point where $v_l \to 0$ [6]. But in our system the dependence of v_l on n^0 is so strongly nonlinear—another effect of fractionation, see inset of Fig. 1—that the resulting cloud point estimates would have very large error bars. Indeed, on a linear plot of v_l versus n^0 as shown in Fig. 1(a) the effects of the particle-size cutoff σ_c, which our more careful analysis reveals (see Fig. 3 below), are essentially invisible.

To make progress, we analyze the finite-size scaling of $p(n)$. As the linear system size L grows at fixed n^0 and T, the peaks in $p(n)$ will narrow around the densities of gas and liquid, respectively, and the size distributions averaged over configurations from each peak will tend to those in the coexisting phases. The ratio $r = v_l/v_g$ is determined by the difference in the grand potential; this is directly related to the pressure P so that $r = \exp(\beta L^d \Delta P)$ for large L where $\beta = 1/k_B T$ and $\Delta P = P_l - P_g$. The criterion for stable coexistence at given fixed n^0 is that r must have a finite value as $L \to \infty$; the pressure difference then has to scale as $\Delta P \sim L^{-d}$ except in the special case $r = 1$ (see above).

For finite L, metastable coexistence can still be observed in the density region $n^0 < n^0_{cl}$ where $\Delta P = O(1)$, but here r will be exponentially small. Figure 2 shows this effect clearly: r is independent of L for sufficiently large n^0, but the curves depart rapidly from each other (note the log scale) for smaller n^0. The cloud point separates the two regimes, permitting the estimate $n^0_{cl} \approx 0.0825 \pm 0.0005$ for the parameters shown in the figure. To derive a method that can estimate n^0_{cl} even from data for only a single system size L, we use the fact that ΔP is $O(1)$ and scales linearly with $n^0 - n^0_{cl}$ to leading order near the cloud point, and hence $\ln r \sim L^d(n^0 - n^0_{cl})$. This applies for $n^0 < n^0_{cl}$, while above n^0_{cl} one has $\ln r = O(1)$. Thus the derivative $(\partial/\partial n^0)\ln r$ should drop from an $O(L^d)$ plateau to $O(1)$ around $n^0 = n^0_{cl}$. In the second derivative $-(\partial/\partial n^0)^2 \ln r$ this drop will manifest itself as a peak. A smooth derivative

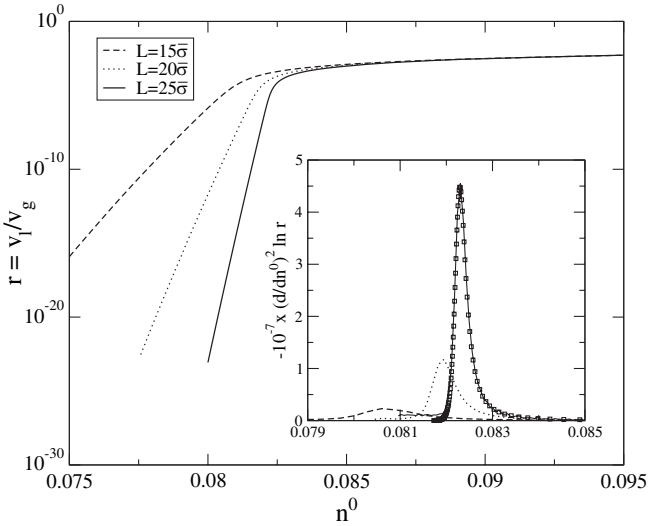

FIG. 2. Ratio r of liquid to gas fractional volumes on approach to the cloud point at $T = T_c$ for $\sigma_c = 1.4$. The inset shows the (negative, scaled) second derivative of $\ln r$ with respect to n^0. The peak position gives an estimate of the cloud point density. Squares indicate the scaled master curve (1).

can be extracted from simulation data using histogram reweighting, and the peak position then serves as an estimate for $n_{\rm cl}^0$. This is shown in the inset of Fig. 2, and gives $n_{\rm cl}^0 \approx 0.0823$ from the largest L, consistent with our earlier estimate derived from comparing data for different L.

The above arguments can be formalized using the results of [11], which pertain to the monodisperse case but which we have generalized to polydisperse systems [12]. We find that for large L the second-derivative plot approaches a *universal* master curve

$$-\left(\frac{\partial}{\partial \tilde{n}^0}\right)^2 \ln r = \frac{z}{(1+z)^3}, \qquad \tilde{n}^0 = z + \ln z, \qquad (1)$$

parametrized by z. The scaled parent density is defined here as $\tilde{n}^0 = aL^d(n^0 - n_{\rm cl}^0) + \ln(bL^d n_{\rm cl}^0)$ with a and b system-specific dimensionless scale factors. This scaling implies that the cloud point estimate from the peak position has finite-size corrections of order $L^{-d}\ln L$, while the peak width and height scale as L^{-d} and L^{2d}, respectively. Our data are consistent with the width and height scaling and with the dominant L^{-d} dependence of the peak shifts [12]. The master curve (1), appropriately scaled, is overlaid onto the largest-L data in Fig. 2 (inset) and shows excellent agreement.

Figure 1 shows that the metastable liquid peak in $p(n)$ persists until well below the cloud point $n_{\rm cl}^0$. The point at which it disappears marks the effective spinodal where the liquid is unstable to small density fluctuations. The parent density $n_{\rm sp}^0$ where this occurs should tend to $n_{\rm cl}^0$ as L grows large, according to $n_{\rm cl}^0 - n_{\rm sp}^0 \sim L^{-3/4}$ [13]. Spinodals in monodisperse systems are conventionally characterized by the density of the phase that becomes unstable, which is located inside the region where phase separation occurs. Here we use instead the density $n_{\rm sp}^0$ of the coexisting *stable* phase, which is outside this region. This is a more meaningful representation in the polydisperse context since only the stable (majority) phase has the parental size distribution, while that of the metastable (minority) phase is determined indirectly via chemical potential equality.

Equipped with a systematic method for determining cloud points, we now consider the overall phase diagram of our system, the interparticle potential of which takes the Lennard-Jones form:

$$u_{ij} = \epsilon_{ij}[(\sigma_{ij}/r_{ij})^{12} - (\sigma_{ij}/r_{ij})^6] \qquad (2)$$

with $\epsilon_{ij} = \sigma_i\sigma_j$, $\sigma_{ij} = (\sigma_i + \sigma_j)/2$ and $r_{ij} = |\mathbf{r}_i - \mathbf{r}_j|$. The potential was truncated for $r_{ij} > 2.5\sigma_{ij}$, and no tail corrections were applied. The diameters σ are drawn from a (parental) Schulz distribution $f^0(\sigma) \propto \sigma^z \exp[(z+1)\sigma/\bar{\sigma}]$, with a mean diameter $\bar{\sigma}$ which sets our unit length scale. We chose $z = 50$, corresponding to a moderate degree of polydispersity: the standard deviation of particle sizes is $\delta \equiv 1/\sqrt{z+1} \approx 14\%$ of the mean. The distribution $f^0(\sigma)$ was limited to within the range $0.5 < \sigma < \sigma_c$. The upper cutoff σ_c serves to prevent the appearance of arbitrarily large particles in the simulation, but would also be expected in experiment because in the chemical synthesis of colloid particles, time or solute limits restrict the maximum particle size [14].

We complement the simulations with theoretical phase behavior calculations, following closely our study of the purely size-polydisperse case [6]. An accurate expression for the excess free energy of a polydisperse hard sphere fluid accounts for the repulsive interactions. To this is added a van der Waals term that represents the attractive part of the u_{ij}. It scales as

$$\int d\sigma d\sigma' \rho(\sigma)\rho(\sigma')(\sigma\sigma')(\sigma+\sigma')^3, \qquad (3)$$

where the factors $\sigma\sigma'$ and $(\sigma+\sigma')^3$ arise, respectively, from the size dependence of the interaction amplitude ϵ_{ij} and the interaction range σ_{ij}. Multiplying out gives an expression involving only the moment densities $\int d\sigma \rho(\sigma)\sigma^i$ with $i = 1, \ldots, 4$. Since the repulsive part of the excess free energy has a similar moment structure, the moment free energy (MFE) method [15] can be used for accurate numerical prediction of phase behavior [6].

Figure 3 shows cloud curves for upper size cutoff $\sigma_c = 1.4$ and 1.6 as obtained from the GCE simulations. A strong σ_c dependence is seen even though both values of σ_c are far in the tail of the parent distribution. This is attributable to very strong fractionation effects (Fig. 4): despite particle sizes around σ_c being very rare in the parent, they occur in significant concentration in the shadow liquid. Physically, since large particles interact more strongly, their presence leads to a substantial free

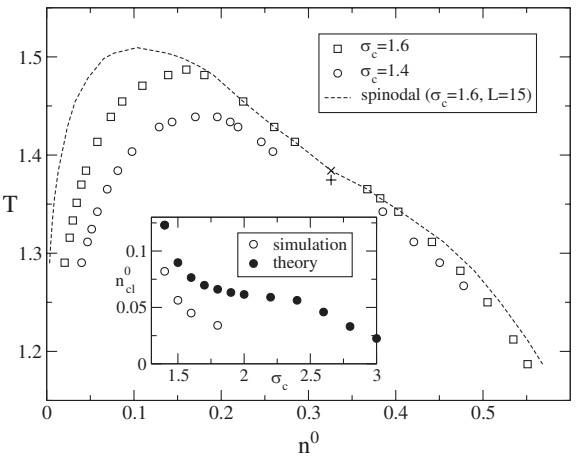

FIG. 3. Comparison of cloud curves for $\sigma_c = 1.4$ and $\sigma_c = 1.6$. The critical points for $\sigma_c = 1.6(\times)$ and $\sigma_c = 1.4(+)$ are marked. Also shown is the effective spinodal (limit of metastability) for $\sigma_c = 1.6$ and $L = 15\bar{\sigma}$. The inset displays the variation of the gas cloud point density $n_{\rm cl}^0$ at $T = T_c$ as a function of σ_c, as obtained from GCE simulations (open symbols) and MFE theory (filled symbols).

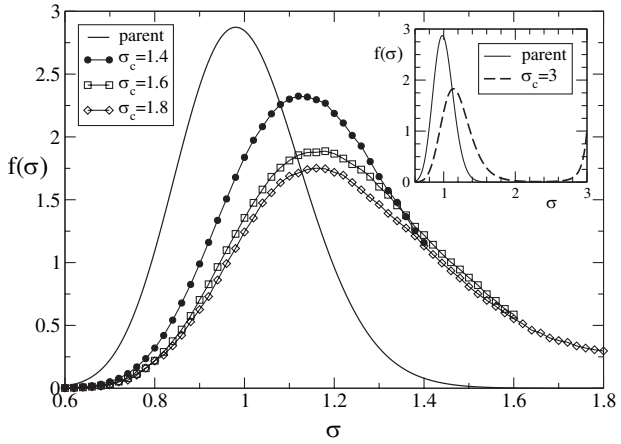

FIG. 4. Size distributions $f(\sigma)$ in the liquid shadow phase distributions at $T = T_c$ for $\sigma_c = 1.4, 1.6, 1.8$, together with the parent distribution $f^0(\sigma)$. Inset: MFE theory prediction for larger cutoff $\sigma_c = 3$; note the second peak in the shadow distribution.

energy gain at the shorter interparticle separations of the liquid.

One is led to enquire whether the gas phase cloud point density would eventually tend to a nonzero limit as σ_c is increased. The inset of Fig. 3 shows the simulation results and theoretical predictions. The former exhibit a further strong decrease of n_{cl}^0 by $\approx 25\%$ between $\sigma_c = 1.6$ and 1.8; the latter suggest that this trend continues and that the cloud point density tends to zero for large σ_c. Such an unusual effect has previously been seen in theoretical studies of polydisperse hard rods with wide length distributions [16] and is also predicted to occur in solid-solid phase separation of polydisperse hard spheres [17], though only for large σ_c and distributions with fatter than exponential tails. Here the decrease of n_{cl}^0 is clear even for σ_c of $O(1)$, i.e., of the same order as $\bar{\sigma}$, and scaling estimates suggest that cutoff effects occur for any size distribution with tails heavier than a Gaussian [12].

The physical origin of the decrease of n_{cl}^0 to zero is the appearance (for large σ_c) of a second peak in the shadow phase size distribution near σ_c (Fig. 4, inset). As with the hard rods, we expect this second peak to eventually dominate as σ_c increases so that the shadow phase consists of ever more strongly interacting particles whose sizes are concentrated near σ_c. We speculate that, as a consequence, there exists some cutoff for which the shadow phase liquid freezes into a quasimonodisperse crystal phase. Indeed, our simulations provide evidence for this scenario: for the large cutoff $\sigma_c = 2.8$ the liquid spontaneously freezes to an fcc crystal structure [12]. Although we observe this only for small n^0 values close to the effective spinodal point, it seems likely that, for σ_c values larger than those presently accessible to simulations, the freezing will occur from the stable liquid phase.

Finally, with regard to the cloud curves as a whole (Fig. 3), we note that significant cutoff-dependent shifts occur only for densities below the critical density. This is consistent with our interpretation above: for higher densities, the shadow phase is a gas of *lower* density than the parent. In this, the concentration of large particles is *suppressed* and that of small particles negligibly enhanced because of their weak interactions. The shadow size distributions are therefore concentrated well within the range $0.5, \ldots, \sigma_c$ (data not shown) so that no cutoff dependence arises.

In summary, the task of accurately locating cloud points of polydisperse fluids via simulation is severely complicated by fractionation effects. We have presented a generally applicable finite-size scaling method that addresses this problem. Application to a model polydisperse fluid reveals the cloud curve to be highly sensitive to the presence of very rare large particles. Such effects imply that in experiments on polydisperse fluids (see, e.g., [4]) it may be important to monitor and control carefully the tails of the size (or charge, etc.) distribution. Otherwise undetected differences could lead to large sample-to-sample fluctuations in the observed phase behavior.

[1] G. H. Fredrickson, Nature (London) **395**, 323 (1998).
[2] R. M. L. Evans, D. J. Fairhurst, and W. C. K. Poon, Phys. Rev. Lett. **81**, 1326 (1998).
[3] K. Ghosh and M. Muthukumar, Phys. Rev. Lett. **91**, 158303 (2003).
[4] B. H. Erné *et al.*, Langmuir **21**, 1802 (2005).
[5] P. Sollich, J. Phys. Condens. Matter **14**, R79 (2002).
[6] N. B. Wilding, M. Fasolo, and P. Sollich, J. Chem. Phys. **121**, 6887 (2004).
[7] R. Kita, K. Kubota, and T. Dobashi, Phys. Rev. E **56**, 3213 (1997).
[8] L. Bellier-Castella, H. Xu, and M. Baus, J. Chem. Phys. **113**, 8337 (2000).
[9] N. B. Wilding, J. Chem. Phys. **119**, 12 163 (2003); N. B. Wilding and P. Sollich, J. Chem. Phys. **116**, 7116 (2002).
[10] B. A. Berg and T. Neuhaus, Phys. Rev. Lett. **68**, 9 (1992).
[11] C. Borgs and W. Janke, Phys. Rev. Lett. **68**, 1738 (1992); C. Borgs and R. Kotecky, Phys. Rev. Lett. **68**, 1734 (1992).
[12] N. B. Wilding, M. Fasolo, and P. Sollich (unpublished).
[13] K. Binder, Physica (Amsterdam) **319A**, 99 (2003).
[14] L. Kvitek *et al.*, J. Mater. Chem. **15**, 1099 (2005).
[15] P. Sollich, P. B. Warren, and M. E. Cates, Adv. Chem. Phys. **116**, 265 (2001).
[16] A. Speranza and P. Sollich, J. Chem. Phys. **118**, 5213 (2003).
[17] M. Fasolo and P. Sollich, Phys. Rev. E **70**, 041410 (2004).